Comptes Rendus
Géoscience — Sciences de la Planète
Supplementary material to the article available at:
https://doi.org/10.5802/crgeos.233

Supplementary material: Molecular fossils of Aptian–Albian blue marls of the Vocontian Basin (France), depositional conditions and connections to the Tethys Ocean

Armelle Riboulleau *, [a], Melesio Quijada [a], Alexis Caillaud [a], François Baudin [b], Jean-Noël Ferry [c] and Nicolas Tribovillard [a]

[a] Laboratoire d'Océanologie & Géosciences, Université de Lille, UMR LOG 8187 Univ Lille-CNRS-ULCO-IRD, 59000, Lille, France

[b] Sorbonne Université, CNRS, ISTeP, 75005, Paris, France

[c] TOTAL S.A., CSTJF, 64000 Pau, France

E-mails: armelle.riboulleau@univ-lille.fr (A. Riboulleau), melesioquijada@gmail.com (M. Quijada), caillaud.alexis@gmail.com (A. Caillaud), francois.baudin@sorbonne-universite.fr (F. Baudin), jean-noel.ferry@total.com (J.-N. Ferry), nicolas.tribovillard@univ-lille.fr (N. Tribovillard)

Not yet published

Supplementary table 1. Biomarker ratios. See Excel file.

Supplementary text 1. Presentation of the studied OLs

The Goguel Level is several meters thick and generally constituted of 6 dark-colored laminated sublevels separated by shales (Supplementary Figure S2), recognizable in a large part of the Vocontian Basin [Bréhéret, 1995, Friès, 1986]. TOC values vary within the Goguel Level and laterally within the basin, but maximum TOC values around 4% are observed and the kerogen is classified as type II [Bréhéret, 1995].

The Niveau Noir comprises four doublets of decimetric dark-colored and unlaminated marls (Supplementary Figure S2). TOC values, ranging between 0.7 and 1.2%, are slightly above those of hemipelagic marls [Bréhéret, 1995]. The low HI values (maximum 120 mgHC/gTOC) suggest degraded marine OM with possible terrestrial contribution [Bréhéret, 1995].

The Fallot Interval comprises six bundles of two to three dark-colored and laminated decimetric levels, which are more or less regularly spaced along a ~22 m-thick sequence of grey marls (Supplementary Figure S2). Fine turbidites are present, particularly in the upper part. The TOC content reaches maximum values around 2% in a few levels but is closer to 1% in the other levels. HI values are generally close to 100 mgHC/gTOC, but maximum values of 200 mgHC/gTOC are observed in the organic-richest levels [Bréhéret, 1995].

* Corresponding author.

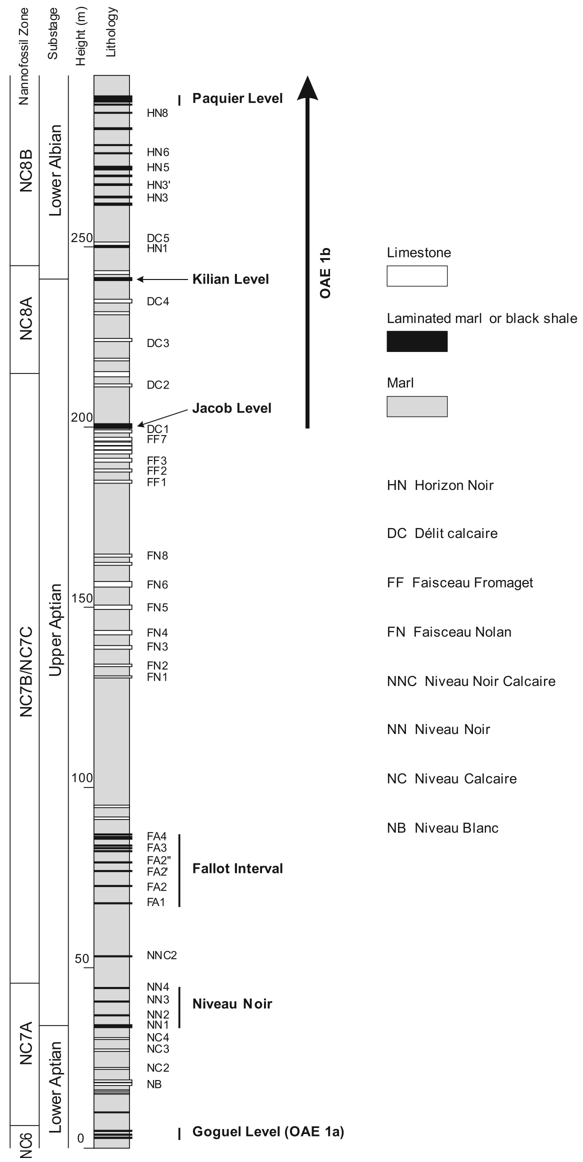

Supplementary Figure S1. Synthetic lithological log of the Blue Marls Formation in the studied interval [modified from Herrle et al., 2010 and Kennedy et al., 2017]. Names of regional marker beds follow the terminology of Bréhéret [1995].

The Jacob Level is approximately 1.5 m-thick and is made of two levels of dark, laminated and fissile marls, several decimeters-thick each (Supplementary Figure S2). The TOC values of the Jacob Level fluctuate between 1 and 2%, while maximum HI values reach 300 mgHC/gTOC [Bréhéret, 1995, Heimhofer et al., 2006].

The Kilian Level is an approximately one-meter-thick level of dark-colored and fissile clays to marls (Supplementary Figure S2). TOC content is rarely higher than 3% [Bréhéret, 1995] and maximum HI values reach 150 mgHC/gTOC.

The Paquier Level is several meters-thick and constituted of six pluridecimetric units of dark colored paper shales (Supplementary Figure S2). A marker limestone bed, named horizon α, is generally present in the upper part of the Paquier Level. The Paquier Level is recognizable in a large part of the Vocontian Basin [Bréhéret, 1995, Friès, 1986]. Generally, TOC values range between 2 and 6%, while the HI values range between 100 and ~550 mgHC/gTOC, though values up to 780 mgHC/gTOC have been locally observed [Benamara et al., 2020, Bréhéret, 1995, Tribovillard and Gorin, 1991]. The kerogen is mainly type II, and HI values are generally higher towards the margins of the basin [Bréhéret, 1995].

Supplementary text 2. Biomarker analysis

1. Extraction and fractionation

Sixty-four samples were selected for biomarker analysis. Information on these samples is given in Supplementary Figure S2. Between 50 and 70 g of powdered dry sediments were extracted using a mixture of dichloromethane (DCM) and methanol (MeOH) 2:1 v/v means of an accelerated solvent extractor (ASE 300, Dionex) at a pressure of 1×10^7 Pa and a temperature of 80 °C, three times for 5 min. The resulting total extracts were rotary-evaporated to dryness at 40 °C. The extracts were recovered with cyclohexane (maltenes-like fraction) and separated over an activated silica column using cyclohexane (CYHA) to recover the aliphatic fraction, a mixture of CYHA/DCM 2:1 (v/v) to recover the aromatic fraction, and a mixture of DCM/MeOH 2:1 (v/v) to recover the most polar fraction. Only the aliphatic and aromatic fractions were analyzed.

2. Gas chromatography—mass spectrometry

The analyses were performed at the University of Lille (PC2A Laboratory UMR 8522 CNRS). Briefly, 1 μL of fraction was injected into a Perkin Elmer 680

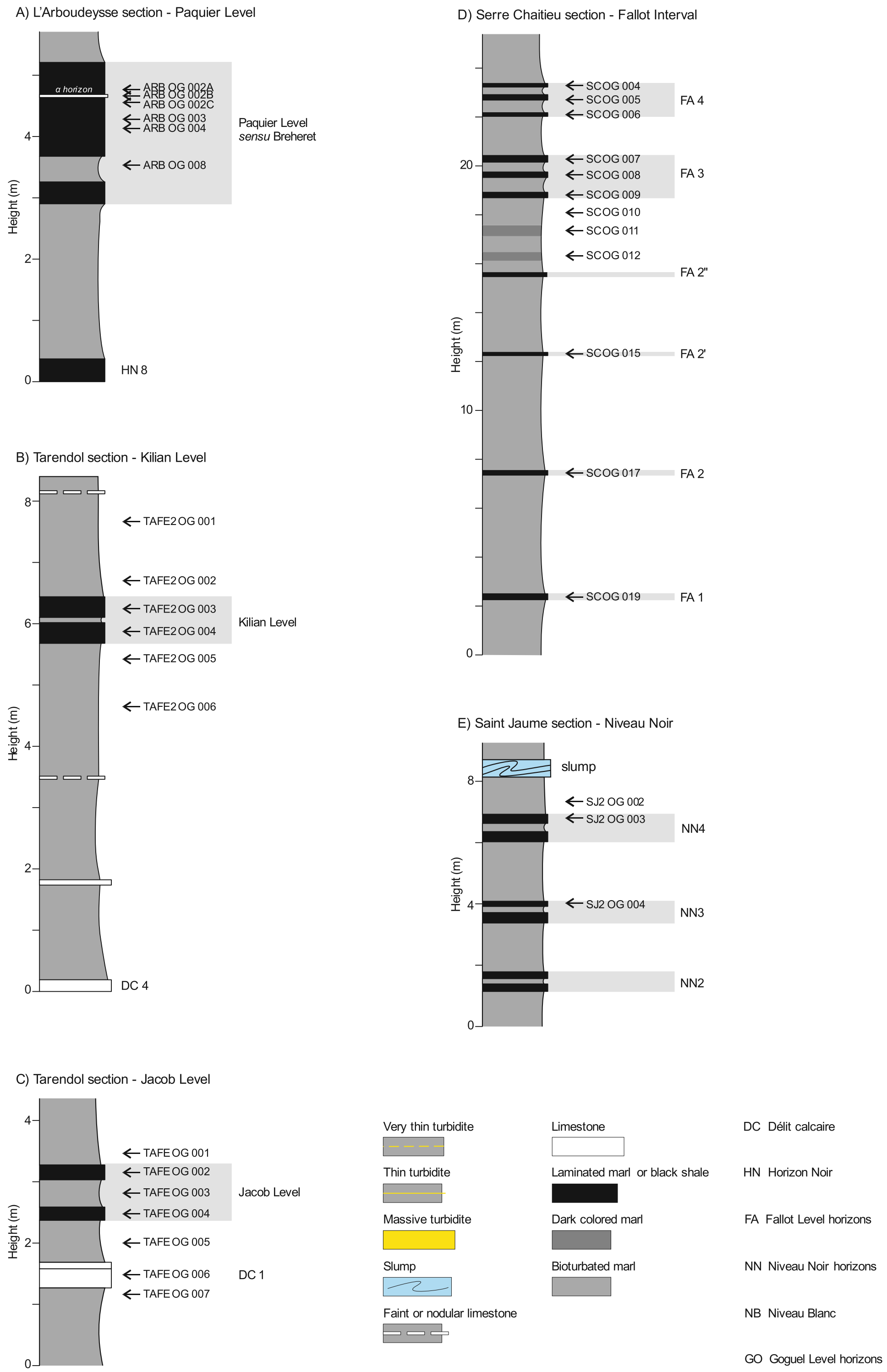

Supplementary Figure S2. Continued on next page.

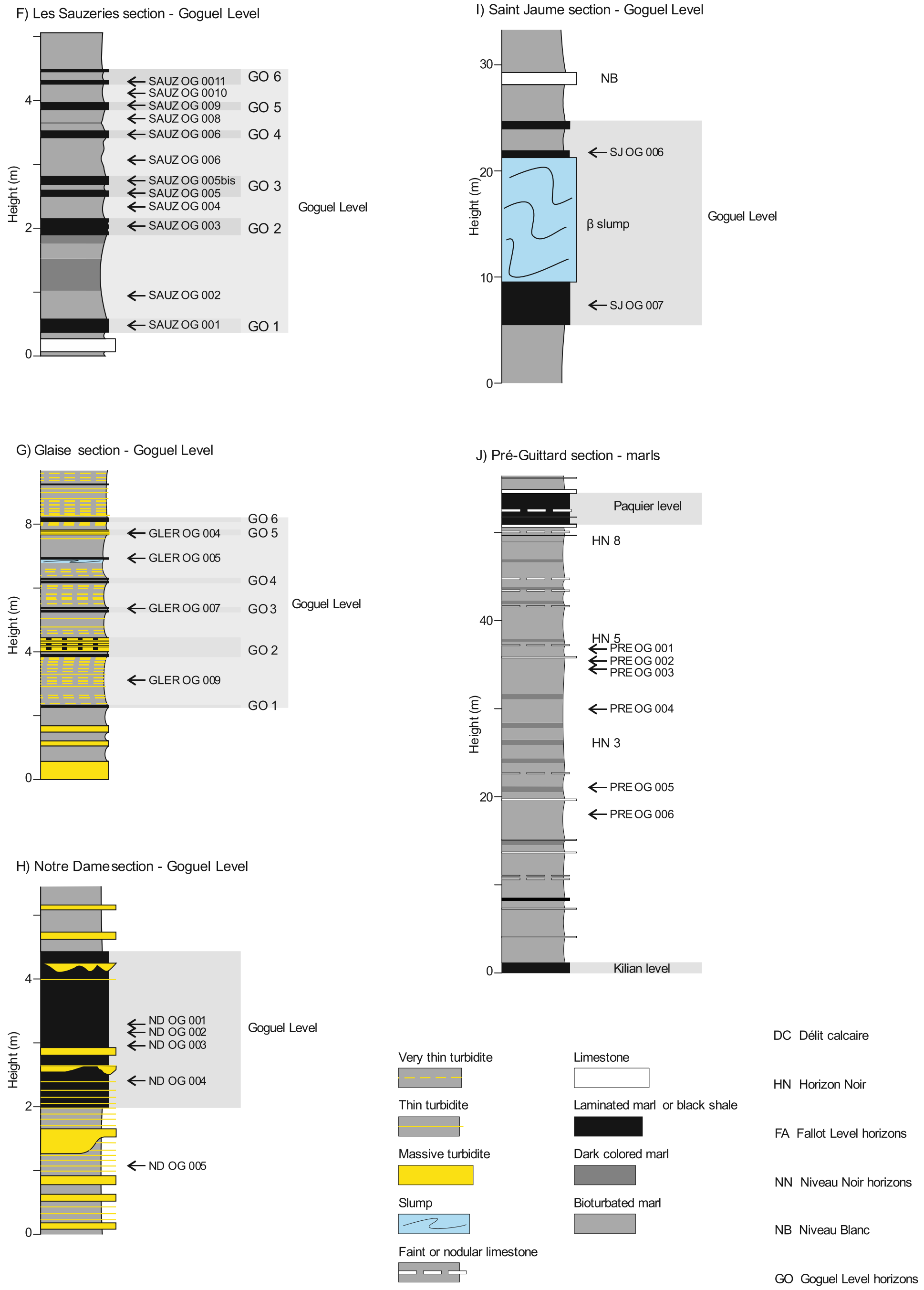

Supplementary Figure S2 (cont.). Lithological log of the studied outcrops and location of the samples selected for biomarker analysis. The names of the sampled horizons follow the terminology of Bréhéret [1995]. Modified from (A) Reichelt [2005]; (B–G) Bréhéret [1995]; (H,I) Friès and Parize [2003], (J) Ait-Itto et al. [2023]. See Figure 1 for the location of outcrops.

gas chromatograph equipped with an auto sampler and coupled with a Perkin Elmer 600C mass spectrometer. Chromatographic conditions were as follow: inlet heated at 250 °C, DB5-MS-UI column initially at 50 °C for 1 min and heated to 310 °C at 4 °C·min^{-1} and maintained 15 min at 310 °C, helium column flow of 1 mL·min^{-1}, splitless mode. Mass spectrometer conditions were as follows: mass scan from m/z 45 to 500, scan time 0.2 s, interdelay scan 0.1 s, ionization energy 70 eV. Compound identification was based on the comparison with NIST mass spectra database and/or on the comparison with retention times of standards and published data. The semi-quantification of compounds and calculation of biomarker ratios was achieved by measuring peak area of selected ion chromatograms. Because of almost coelution of pristane and the n-C_{17} alkane, integration of the peak for each compound was made by deconvolution of the chromatograms using Gaussian peak shapes and least square fitting with an Excel routine.

3. Ions and calculations of biomarker ratios

3.1. *Saturate fraction*

3.1.1. *Alkanes and acyclic isoprenoids*

Pr/nC_{17} = pristane/n-C_{17} alkane (TIC)

Ph/nC_{18} = phytane/n-C_{18} alkane (TIC)

Pr/Ph = pristane/phytane (TIC)

$OEP_{23} = (C_{21} + 6C_{23} + C_{25})/(4C_{22} + 4C_{24})$ [Scalan and Smith, 1970]

$OEP_{27} = (C_{25} + 6C_{27} + C_{29})/(4C_{26} + 4C_{28})$ [Scalan and Smith, 1970]

$CPI = [(C_{25} + C_{27} + C_{29} + C_{31} + C_{33})/(C_{24} + C_{26} + C_{28} + C_{30} + C_{32}) + (C_{25} + C_{27} + C_{29} + C_{31} + C_{33})/(C_{26} + C_{28} + C_{30} + C_{32} + C_{34})]/2$ [Bray and Evans, 1961]

$TAR = (C_{27} + C_{29} + C_{31})/(C_{15} + C_{17} + C_{19})$ [Bourbonniere and Meyers, 1996]

ipr/n = Σ C_{15}-C_{21} regular isoprenoids/Σ C_{15}-C_{21} linear alkanes.

br/n = Σ (C_{15}-C_{24} 2-me- and 3-me-alkanes) × 10/Σ C_{15}-C_{24} linear alkanes

PMIR: pentamethylicosane ratio PMIR = PMI/(PMI + n-C_{22} alkane)

3.1.2. *Regular steranes and diasteranes*

%$C_x = C_x/(C_{27} + C_{28} + C_{29})$ with x = 27–29, using peak areas of 20R-ααα regular steranes (m/z 217)

C_{30} sterane ratio = $C_{30}/(C_{27} + C_{28} + C_{29} + C_{30})$ [Moldowan et al., 1985] using peak areas of 20R-ααα epimers (m/z 217)

The sterane C-20 isomerisation ratio S/(S+R) was calculated for the C_{29} ααα sterane (m/z 217).

The sterane isomerisation ratio at C-14 and C-17 ββ/(ββ + αα) was calculated for the C_{27} 20S and 20R epimers (m/z 372).

%$DC_x = DC_x/(DC_{27} + DC_{28} + DC_{29})$ with x = 27–29, using peak areas of (20R + 20S)-βα diasteranes (m/z 372, 386, and 400, respectively)

The diasterane C-20 isomerisation ratio S/(S+R) was calculated for the C_{27} βα diasterane (m/z 217).

Dia/reg = Σ C_{27} diasteranes/Σ C_{27} regular steranes (m/z 372)

Ster/alk = sum of all isomers of C_{27} to C_{29} diasteranes and steranes (m/z 217) divided by the sum of C_{15} to C_{33} n-alkanes (m/z 57)

3.1.3. *Methylsteranes*

MeSter/Ster: sum of all isomers of C_{28} to C_{30} methylsteranes, including dinosteranes (m/z 231) divided by the sum of all isomers of C_{27} to C_{29} diasteranes and regular steranes (m/z 217).

4MeSter/MeSter = (4Me-C_{28} + 4Me-C_{30})/(2Me-C_{28} + 3Me-C_{28} + 4Me-C_{28} + 2Me-C_{30} + 3Me-C_{30} + 4Me-C_{30}) (m/z 231)

Dino/MeSter = Σ dinosteranes/Σ (C_{28} to C_{30} 2-, 3-, and 4-methylsteranes) (m/z 231)

%3Me-Cx = 3Me-C_x/(3Me-C_{28} + 3Me-C_{29} + 3Me-C_{30}) with x = 28–30 (m/z 231)

EtSter/Ster: sum of all isomers of C_{29} to C_{31} 3β-ethylsteranes (m/z 245) divided by the sum of all isomers of C_{27} to C_{29} diasteranes and regular steranes (m/z 217).

%3Et-Cx = 3Et-C_x/(3Et-C_{29} + 3Et-C_{30} + 3Et-C_{31}) with x = 29–31 (m/z 245)

3.1.4. *Diasterenes and methyldiasterenes*

%C_x Dia:1 = C_x Dia:1/(C_{27} Dia:1 + C_{28} Dia:1 + C_{29} Dia:1) with x = 27–29 using peak areas of (20R + 20S)-10α diaster-13(17)-enes (m/z 257)

C_{30} diasterene ratio: sum of all C_{30} diaster-13(17)-enes epimers divided by the sum of all C_{27} to C_{29} diaster-13(17)-enes epimers (m/z 257)

Dia:1/alk: sum of all epimers of C_{27} to C_{29} diaster-13(17)-enes (m/z 257) divided by the sum of C_{15} to C_{33} n-alkanes (m/z 57)

MeDia:1/Dia:1: sum of all epimers of methyl-diaster-13(17)-enes (m/z 271) divided by the sum of all C_{27} to C_{29} diaster-13(17)-enes epimers (m/z 257)

3.1.5. *Saturated hopanoids (m/z 191)*

The hopane C-22 isomerisation ratio S/(S+R) was calculated for the C_{31} $\alpha\beta$ hopane.

The hopane to moretane isomerisation ratio $\beta\alpha/(\beta\alpha+\alpha\beta)$ was calculated for the C_{29} and C_{30} compounds. Because of coelution of $\beta\alpha$ C_{30} and $\beta\beta$ C_{29} hopanes, the C_{30} $\beta\alpha/(\beta\alpha+\alpha\beta)$ ratio can be overestimated.

Ts/(Ts+Tm) = 18α-22,29,30-trisnorneohopane/(18α-22,29,30-trisnorneohopane + 17α-22,29,30-trisnorhopane)

C_{27}/C_{30} hopane = $\alpha\beta C_{27}/\alpha\beta C_{30}$

C_{29}/C_{30} hopane = $\alpha\beta C_{29}/\alpha\beta C_{30}$

$C_{31}R/C_{30}$ = 22(R)-$\alpha\beta C_{31}/\alpha\beta C_{30}$ [Peters et al., 2005]

C_{35} HHI = C_{35} 22(S + R)-$\alpha\beta\times 100/\Sigma$ C_{31} to C_{35} 22(S + R)-$\alpha\beta$ [Peters and Moldowan, 1991]

Ster/Hop: sum of all epimers of C_{27} to C_{29} diasteranes and regular steranes (m/z 217) divided by the sum of all C_{27} to C_{35} hopanoids (m/z 191).

Hop/Alk: sum of all C_{27} to C_{35} hopanoids (m/z 191) divided by the sum of C_{15} to C_{33} *n*-alkanes (m/z 57)

2-MHI = C_{31} 2α(Me)-$\alpha\beta$ hopane/(C_{30} $\alpha\beta$ hopane + C_{31} 2α(Me)-$\alpha\beta$ hopane) with C_{30} $\alpha\beta$ hopane integrated on m/z 191 and C_{31} 2α(Me)-$\alpha\beta$ hopane integrated on m/z 205 [Ando et al., 2022]

2MPH/STN = C_{31} 2α(Me)-$\alpha\beta$ hopane/(Σ C_{27}-C_{29} 20R-ααα steranes) with C_{31} 2α(Me)-$\alpha\beta$ hopane integrated on m/z 205 and steranes integrated on m/z 217 [Ando et al., 2022]

3.2. *Aromatic fraction*

3.2.1. *Triaromatic steroids*

Because of the coelution of C_{26}R and C_{27}S triaromatic steroids (TA, m/z 231), the relative abundance of C_{26}, C_{27}, and C_{28} TA was determined using the assumption that the S/R isomerisation ratio was the same as the one determined for the C_{28} for all chain lengths.

%C_x TA = C_x TA/(C_{26} TA + C_{27} TA + C_{28} TA) with $x = 26$–28 using peak areas of (20R + 20S) triaromatic steroids (m/z 231)

Because of the numerous coelutions of methyl-triaromatic steroids (MeTA, m/z 245), the relative abundance of compounds was determined using the assumption that the 2-+3-MeTA/4-MeTA ratio was the same as the one determined for the (20S-C_{28} + 20R-C_{27}) peaks, for all chain lengths.

MeTA/TA: sum of all C_{27}-C_{29} MeTA and TA dinosteroids (m/z 245) divided by the sum of all C_{26}-C_{28} TA (m/z 231)

4-MeTA/MeTA: 4-methyl-C_{28}S TA divided by the sum of 2-, 3-, and 4-methyl C_{28}S TA (m/z 245)

TAD/MeTA: sum of TA dinosteroids divided by the sum of all isomers of C_{27} to C_{29} 2-, 3-, and 4-Me TA (m/z 245)

TADS = 100× (TA dinosteroids except D6)/[(C_{26}—C_{27} TA steroids) + (A-ring methyl C_{27}—C_{28} TA steroids) + (TA dinosteroids except D6)] [Ando et al., 2017]

C_{27} TAS = 100× [C_{27} TA steroids)/[(C_{26}—C_{27} TA steroids) + (A-ring methyl C_{27}—C_{28} TA steroids) + (TA dinosteroids except D6)] [Ando et al., 2017]

3.2.2. *Other aromatic compounds*

HPI = [cadalene (m/z 183) + ip-iHMN (m/z 197) + retene (m/z 219)]/1,3,6,7-TeMN (m/z 184) [van Aarssen et al., 2000]; ip-iHMN: 6-isopropyl-1-isohexyl-2-methyl-naphthalene; 1,3,6,7-TeMN: 1,3,6,7-tetramethylnaphthalene

HPI* = [cadalene (m/z 183) + ip-iHMN (m/z 197) + retene (m/z 219)]/phenanthrene (m/z 178)

HPP = retene (m/z 219)/[cadalene (m/z 183) + retene (m/z 219)] [van Aarssen et al., 2000]

AI/P = sum of aryl isoprenoids (m/z 133+134)/phenanthrene (m/z 178)

Aryl isoprenoids ratio, AIR = (C_{13}-C_{17})/(C_{18}-C_{22}) aryl isoprenoids (m/z 133+134) [Schwark and Frimmel, 2004]

PAH/P = sum of PAHs (m/z 202 + 228 + 252 + 276 + 300)/phenanthrene (m/z 178)

DBF/P = 10× dibenzofuran (m/z 168)/phenanthrene (m/z 178)

MPR = 2-MP/1-MP with x-MP: x-methyl-phenanthrene (m/z 192) [Radke et al., 1982b]

MPI 1 = 1.5 × (2-MP + 3-MP)/(P + 1-MP + 9-MP) with P: phenanthrene (m/z 178) and x-MP: x-methyl-phenanthrenes (m/z 192) [Radke et al., 1982a]. Response factors were applied in order to take account of the use of mass spectrometry.

Supplementary text 3. Biomarker distribution

1. Linear and branched alkanes

The samples from the Paquier Level excepted, the saturated fractions are dominated by a series of linear alkanes (*n*-alkanes) ranging from C_{13} to C_{35} in most cases. The distribution of *n*-alkanes is unimodal and presents a maximum in C_{16} or C_{17} (Figure 3). In most of the samples, long chain *n*-alkanes present a predominance of odd numbered compounds in the range C_{23}–C_{33} (Supplementary Table 1). Most of the samples have a terrestrial *vs.* aquatic ratio [TAR; Bourbonniere and Meyers, 1996] value lower than 0.4, reflecting the low contribution of long chain alkanes. Nevertheless a few marl samples have a TAR value higher than 1 (Supplementary Table 1). The odd predominance in long alkanes is absent in the samples of the Goguel Level at les Sauzeries and Glaise (OEP_{27} values close to 1), while the highest values of the OEP_{27} are observed in the Fallot Interval and Paquier Level.

Series of 2-methyl- and 3-methyl-alkanes are observed in most of the samples. Their distribution generally ranges between C_{15} and C_{21} with a maximum around C_{17}, but longer chain lengths, up to C_{27} are present in a few samples. High relative abundances of these branched alkanes are observed in a sample from the Paquier Level, in the Niveau Noir, as well as in the Goguel Level at Saint Jaume and Notre-Dame (Supplementary Table 1). Conversely, low abundances are observed in the Fallot Interval.

2. Acyclic and monocyclic isoprenoids

In most of the samples, acyclic isoprenoids consist in a series of regular isoprenoids ranging from C_{14} to C_{21}, largely dominated by pristane (Pr) and phytane (Ph) with C_{17} in minor abundance. The ratio of regular isoprenoids to *n*-alkanes in the C_{15}–C_{21} range (ipr/n ratio) is close to or lower than 1 (Supplementary Table 1). In the Paquier and Jacob Levels, the relative abundance of regular isoprenoids is higher as indicated by the high values of the ipr/n ratio (Supplementary Table 1). However, while the dominant isoprenoid is pristane in the Paquier Level, 2,6,10-trimethyltetradecane (C_{16}) dominates in the samples from the Jacob Level. In addition to the regular linear isoprenoids, the samples from the Paquier Level contain C_{24}–C_{26} tail-to-tail linked irregular isoprenoids i.e. 2,6,15,19-tetramethylicosane (TMI), 2,6,10,15,19-pentamethylicosane (PMI) and 10-ethyl-2,6,15,19-tetramethylicosane (ETMI), as previously described by Vink et al. [1998, Figure 3]. A pentamethylhenicosane (PMH) is also tentatively identified, based on its elution time and mass spectrum (Supplementary Figure S4). Three cyclic compounds with a cyclohexyl ring and an isoprenoid skeleton, ranging from C_{17} to C_{19} previously described by Vink et al. [1998] are also present in significant proportion in the samples of the Paquier Level. In addition, numerous other compounds showing comparable structure were tentatively identified based on the distribution of m/z 83, 97, 111 and 125 fragments (Supplementary Figure S5). These compounds, ranging from C_{14} to C_{20}, are also present in one sample of the Jacob Level.

Most of the samples have a Pr/Ph ratio higher than 1 (Supplementary Table 1). The highest Pr/Ph values, up to 8.6, are observed in the marls samples at Pré-Guittard. By decreasing order of Pr/Ph ratios, the organic levels are the Fallot Interval, Kilian Level, Goguel Level at Saint Jaume, Goguel Level at Notre-Dame, Niveau Noir, Goguel Level at Glaise and les Sauzeries. Only some samples from the Jacob and Paquier Levels, have Pr/Ph values close to or lower than 1 (Supplementary Table 1).

3. Steroids

Mass chromatogram m/z 217 shows the distribution of diasteranes and regular steranes (Supplementary Figure S6). These compounds are present in significant proportion in the samples from the Paquier and Jacob Levels and the Goguel Level at Notre-Dame and Saint Jaume. They are often present in low proportion in the other intervals. The distribution of sterane and diasterane isomers is comparable in most of the samples: presence of the four diastereomers of diasteranes with a predominance of $\beta\alpha$ epimers, steranes dominated by the 20R-$\alpha\alpha\alpha$ epimers followed by the $\beta\alpha\alpha$ epimers. At Glaise and les Sauzeries, the distribution of steranes is marked by the absence of the $\beta\alpha\alpha$ epimers and a high relative abundance of the $\alpha\beta\beta$ epimers. The relative abundance of diasteranes and steranes is generally similar, however, a lower relative abundance of diasteranes is noted in the samples of the Paquier Level (Supplementary Table 1). In terms of chain length, diasteranes distribution is dominated by the

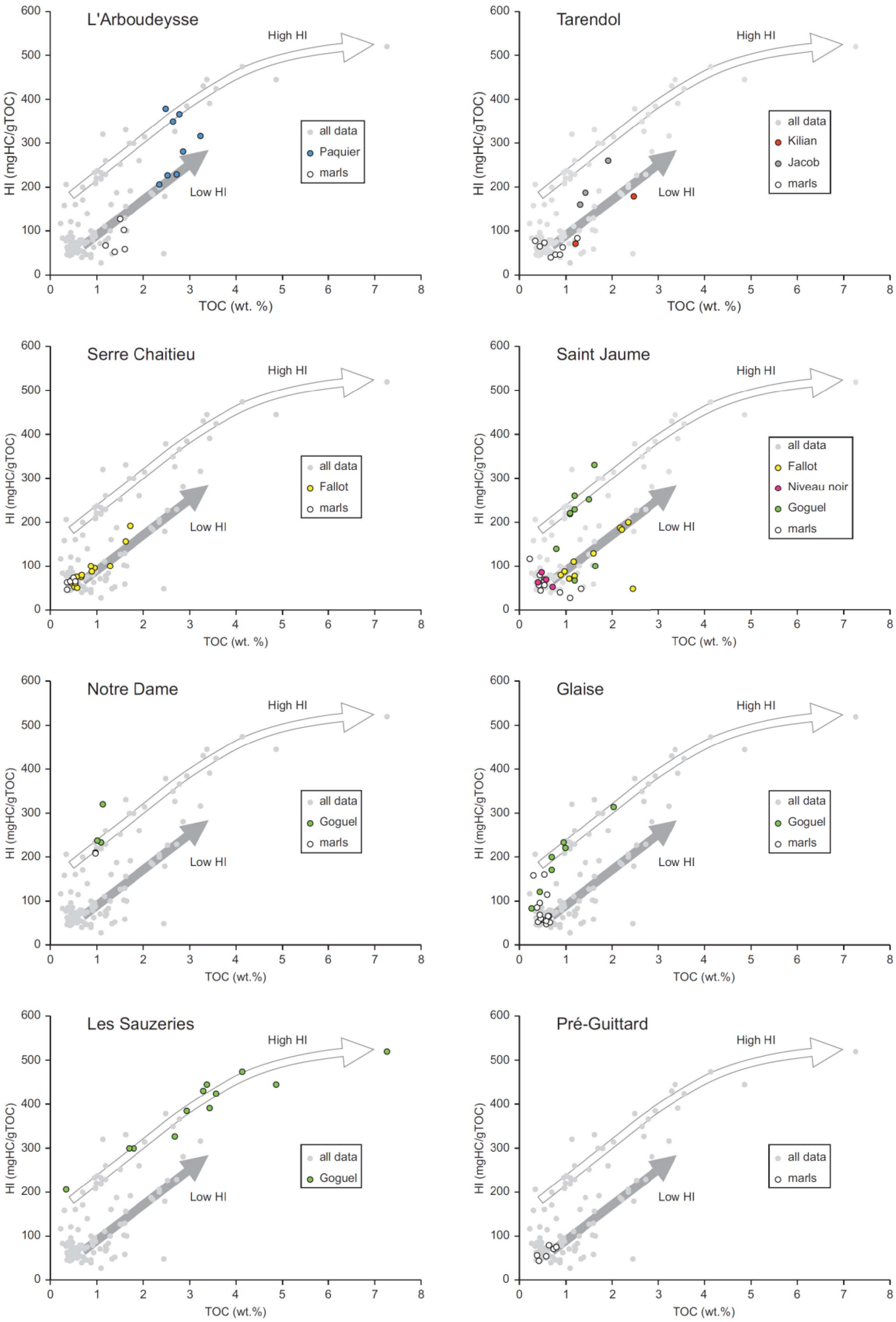

Supplementary Figure S3. Cross plot of the total organic carbon (TOC) content and Hydrogen Index (IH) values for the rock samples of the Blue Marls Formation by section. See Figure 1 for the location of outcrops. The two trends depicted by the arrows are discussed in the main text.

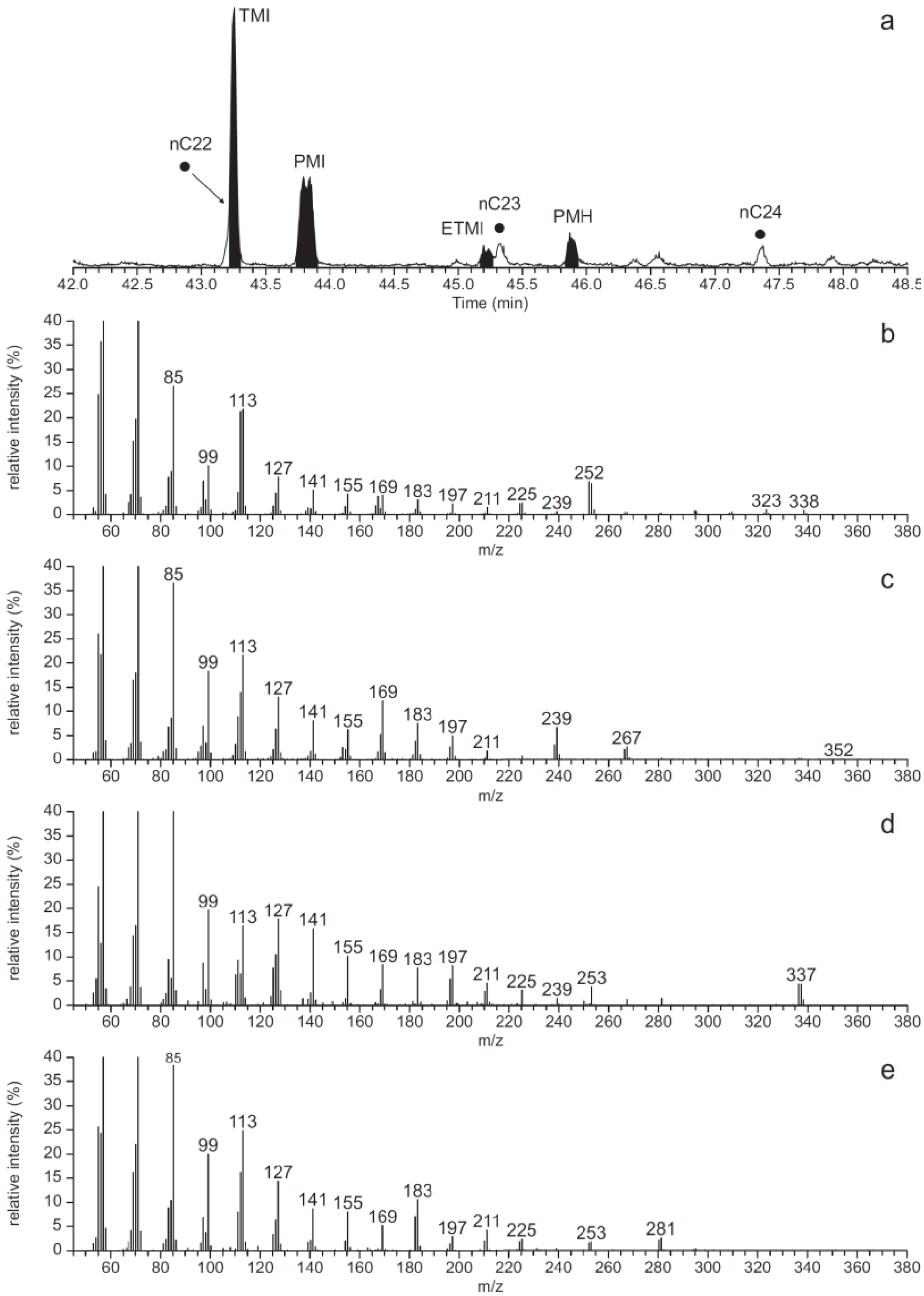

Supplementary Figure S4. (a) Partial mass chromatogram m/z 113 showing the distribution of alkanes and acyclic isoprenoids. (b–e) Mass spectra of 2,6,15,19-tetramethylicosane (TMI, b); 10-ethyl-2,6,15,19-tetramethylicosane (ETMI, c); 2,6,10,15,19-pentamethylicosane (PMI, d); unknown compound tentatively identified as a pentamethylhenicosane (PMH). Sample ARBOG002B, Paquier Level.

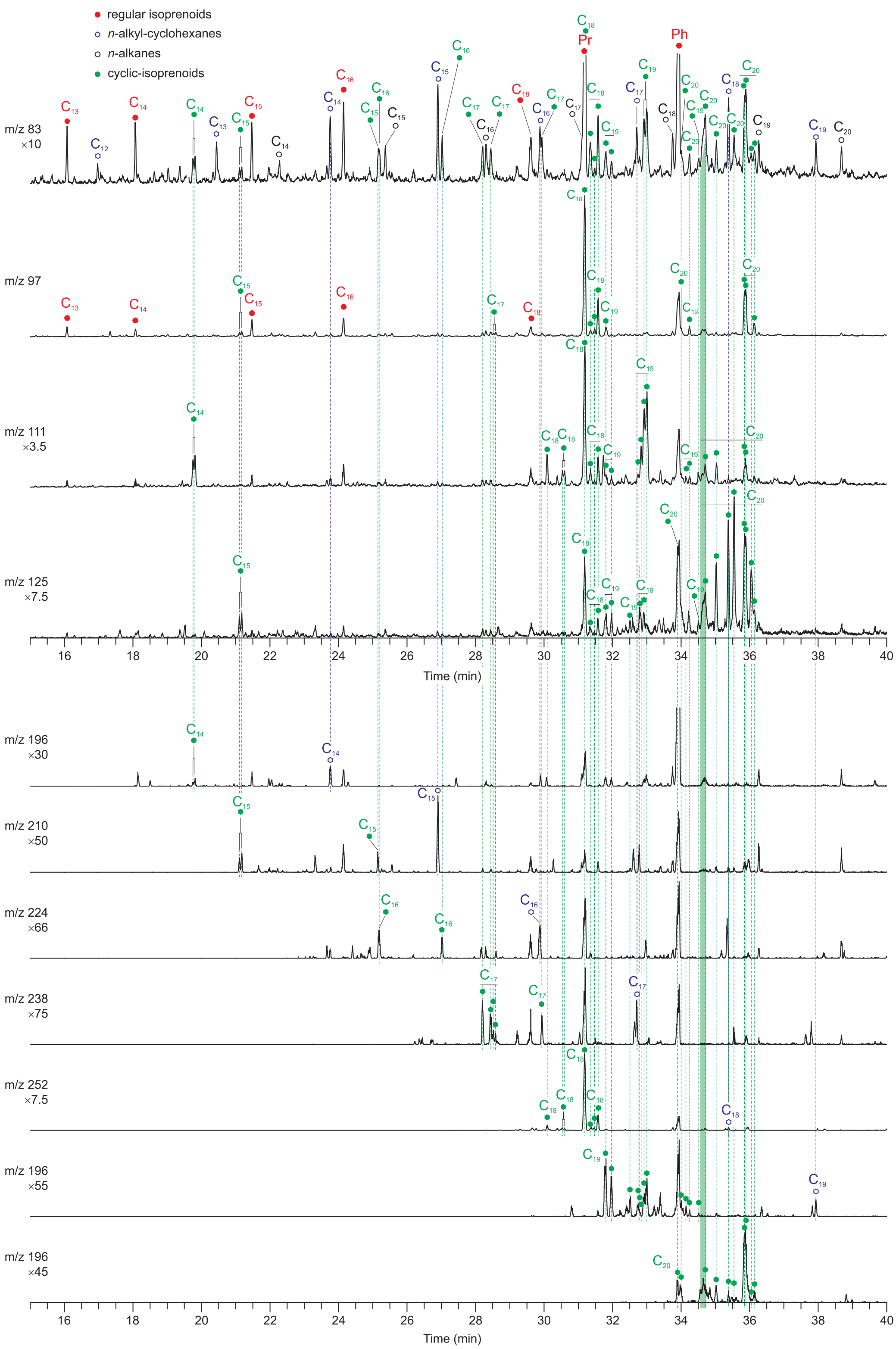

Supplementary Figure S5. Partial mass chromatograms m/z 83, 97, 111, 125, 196, 210, 224, 238, 252, 266, and 280 showing the distribution of C_{14}–C_{20} monocyclic isoprenoids (sample ARBOG002A, Paquier Level).

C_{29} compounds in most of the samples (Supplementary Table 1). In the Paquier Level and Fallot Interval, however, the C_{28} diasteranes are often dominant (Supplementary Table 1). The regular steranes are generally dominated by the C_{29} compounds (Figure 5, Supplementary Table 1). In the Paquier Level, however, C_{27} isomers are the dominant regular steranes. 24-*n*-Propylcholestanes are observed in most of the samples, where they are present in variable proportion. The highest relative abundance of these C_{30} steranes is observed in the Paquier Level, followed by the Goguel Level at les Sauzeries (Supplementary Table 1).

Mass chromatogram m/z 231 shows the distribution of methylsteranes (Supplementary Figure S6). These compounds are present in most of the samples, except marls. In the absence of MS-MS, the identification of methylsteranes was based on careful examination of mass chromatograms m/z 231, 286, 400 and 414 and comparison with different methylsterane patterns published in the literature [Brocks et al., 2003, Chen and Summons, 2001]. The identified methylsteranes mainly correspond to series of 2α-methyl-steranes, 3β-methyl-steranes, and 4α-methyl-steranes. Only 20R-epimers are present. Dinosteranes are also present in minor proportion. The highest relative abundances of methysteranes are observed in the samples of the Kilian and Fallot Levels and associated marls, while very low abundance is observed in the samples of the Goguel Level at les Sauzeries and Glaise. The relative proportion of 2α- and 3β-methyl-steranes is relatively constant, while the proportion of 4α-methyl-steranes varies. Highest proportions of 4α-methyl-steranes are observed in the Paquier Level, and Goguel Level at Notre-Dame and Saint Jaume. The relative abundance of dinosteranes compared to the other methylsteranes is maximum in the Paquier Level. High relative abundances of dinosteranes are also observed in the Goguel Level at Notre-Dame and Saint Jaume, and in a few samples of the Fallot Interval. Mass chromatogram m/z 245 also allows the detection of 3β-ethyl-steranes in several samples (Supplementary Table 1). When present, their distribution in terms of chain length is comparable to that of non-methylated steranes.

Diaster-13(17)-enes and methyldiaster-13(17)-enes are detected in all the samples using mass chromatograms m/z 257 and 271, respectively (Supplementary Figure S7). Their abundance is generally low in the Goguel Level, and particulaly so at les Sauzeries and Glaise sections. Four epimers of diasterenes are present, with a dominance of the 10α epimers (Supplementary Figure S7). In terms of chain length, the distribution of diasterenes is dominated by the C_{29} compounds except in the Paquier Level where C_{27} compounds dominate. 24-*n*-Propylcholestenes are present in low and comparable proportion in most of the samples. Methyldiasterenes mostly correspond to 4-methyldiaster-13(17)-enes, though two unidentified C_{28} methyldiaterenes are observed in several samples (Supplementary Figure S7). Additional C_{30} compounds possibly corresponding to diadinosterenes are also observed in several samples (Supplementary Figure S7).

4. Hopanoids

Hopanes are detected in all the samples using ion chromatogram m/z 191. Their distribution is comparable in most of the samples, except for samples from les Sauzeries and Glaise sections. Hopanes range from C_{27} to C_{35} (C_{28} absent) with a maximum in C_{30} and a progressive decrease of the abundance homohopanes with increasing chain length (Figure S6). The αβ-hopanes are dominant while βα-hopanes (moretanes) are present in minor proportion; ββ-hopanes were also detected in low proportion in many samples. Homohopanes are dominated by the R epimer. Rearanged hopanoids of the Ts series (18α(H)-neohopanes) ranging from C_{27} to C_{30} (C_{28} absent) are present in low proportions. C_{29} and C_{30} neohop-13(18)-enes were present in most of the samples while hop-17(21)-enes were detected in trace proportions. At les Sauzeries and Glaise, hopanes distribution differs by the absence of ββ-hopanes and hopenes, and the low abundance of moretanes. Conversely, 17α(H)-diahopanes from C_{27} to C_{30} (C_{28} absent) are present, though in low proportion. Homohopanes are dominated by the S epimer and traces of long homohopanes (C_{36} and C_{37}) were detected. In addition to these compounds, 2α-methyl-hopanes were detected basing on mass chromatogram m/z 205 (Figure 6). In the absence of MS-MS, compounds identification was based on careful examination of published chromatograms [Brocks et al., 2003, Summons and Jahnke, 1990]. The distribution of 2α-methyl-hopanes ranges from C_{28} to C_{35}, with a maximum in C_{31}. Basied on the

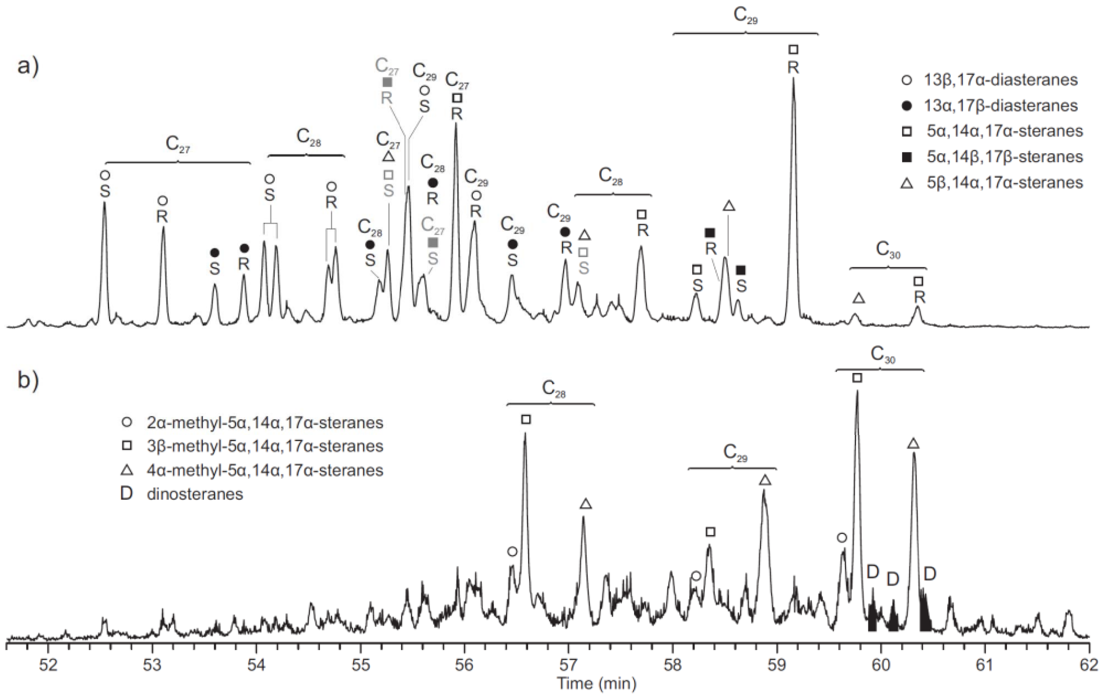

Supplementary Figure S6. Partial mass chromatograms showing the typical distribution of (a) diasteranes and steranes (m/z 217); (b) methylsteranes (m/z 231). Sample NDOG001—Goguel Level. Grey symbol indicates the compound is minor.

2-methylhopane index [2-MHI, *sensu* Ando et al., 2022] the presence of 2α-methyl-hopanes is obvious in most of the studied samples from the Goguel Level (Supplementary Table 1). Conversely, 2α-methyl-hopanes are absent from the extract of most of the marl samples. In the absence of MS-MS, the presence of 2α-methyl hopanes could not be ascertained for all other samples. Nevertheless, if present, their abundance is very low (Supplementary Table 1). 2β-Methyl-hopanes [Summons and Jahnke, 1990] are also present in low proportion in all the samples from Notre-Dame (Figure 6). Traces of C_{31} 3β-methylhopane are also detected in most of the samples (Figure 6).

A series of 8,14-secohopanes is present in low proportion. These compounds are detected through the monitoring of ion m/z 123 [Wang et al., 1990]. Chain lengths range from C_{27} to C_{30} (C_{28} absent) and only one isomer of unknown configuration is observed for each compound. This series is mostly detected in the samples from the Goguel Level, showing the highest proportion in the samples from les Sauzeries section.

5. Other saturated terpenoids

Ion chromatogram m/z 191 also reveals the presence of the 20S and 20R epimers of dammar-13(17)-enes and the 20S and 20R epimers of their saturated counterparts, namely 13β,17α(H)-dammaranes, as identified by [Meunier-Christmann et al., 1991]. These compounds are present in very low proportion and are only observed in the samples of the Paquier Level.

Finally, ion chromatogram m/z 191 also reveals the presence of a series of cheilanthanes ranging from C_{19} to C_{26}. These compounds are present in low proportion in the organic levels and present a similar distribution. Widespread in the samples from the Goguel Level, Niveau Noir, and the Paquier Level, cheilanthanes are more sporadic in the Fallot Interval, and the Jacob and Kilian Levels.

Bicyclic terpenoids ranging from C_{13} to C_{16} are observed in many samples, using ion chromatograms m/z 109, 123, 179, 193 and 207 [Noble, 1986]. For the Niveau Noir, Fallot Interval, Jacob and Killian Levels, the dominant compound generally is 18β(H)-

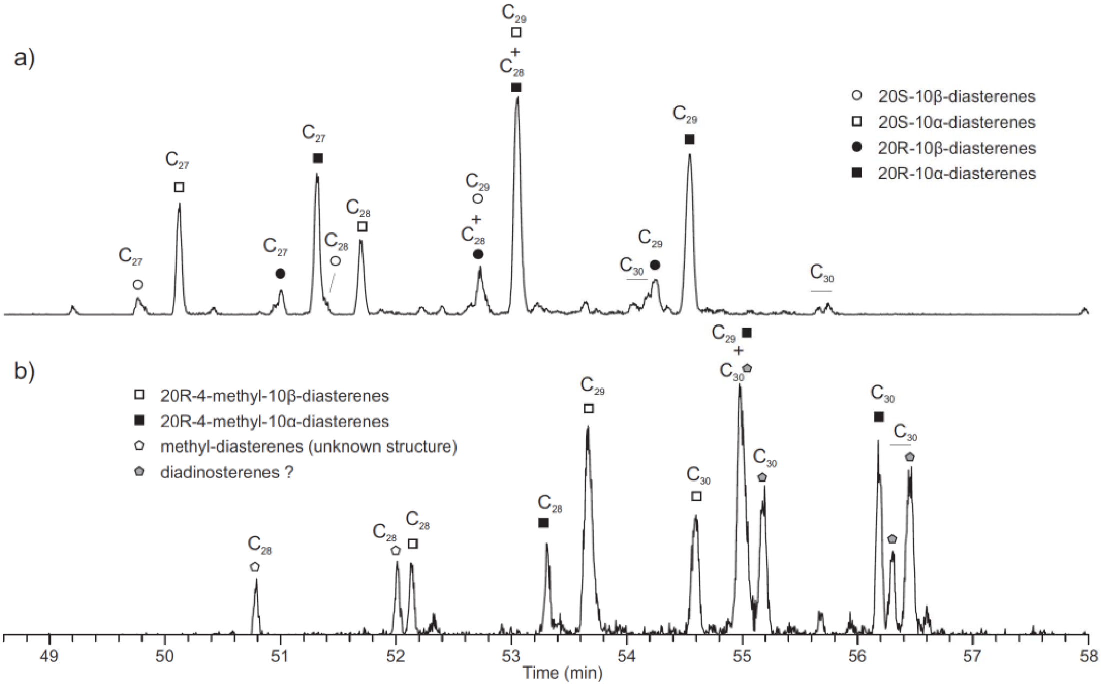

Supplementary Figure S7. Partial mass chromatograms showing the typical distribution of (a) diaster-13(17)-enes (m/z 257) and (b) methyl-diaster-13(17)-enes (m/z 271). Sample TAFE2OG004—Kilian Level.

homodrimane (Supplementary Figure S8b). In the Paquier and Goguel Levels, the dominant compound generally is a C_{14} or a C_{15} bicyclane of unknown origin. A larger variety of bicyclic terpenoids is observed at les Sauzeries and Glaise (Supplementary Figure S8a). This might reflect the higher thermal maturity of the organic matter.

6. Aromatic steroids

Ring-C monoaromatic steroids and their methylated counterparts are observed in all the samples basing on chromatograms m/z 253 and 267, respectively (Supplementary Figure S9). The identification of non-methylated compounds was based on the comparison with elution patterns shown in [Riolo et al., 1986]. The distribution pattern of non-methylated compounds is comparable in most of the samples, dominated by the C_{27}–C_{29} compounds, with a minor contribution of the C_{21} and C_{22} homolgs. In most of the samples, the distribution of isomers is dominated by the rearranged 5β,10β(H)- and 5α,10α(H)- structures (Supplementary Figure S9b). Only in the samples from the Paquier Level does the isomer distribution markedly differ, with a predominance of regular 5β(H),10β- and 5α(H),10α-structures (Supplementary Figure S9a). In the samples from Notre-Dame section, similar contributions of regular and rearranged structures are observed. Though methylated compounds could not be identified, a systematic difference in the distribution patterns is similarly observed between the Paquier Level and other samples (Supplementary Figure S9c,d).

Non-methylated and methylated triaromatic steroids are detected using ion chromatograms m/z 231 and 245, respectively (Supplementary Figure S10). The distribution of non-methylated triaromatic steroids is comparable in most of the samples and is dominated by the C_{26}–C_{28} compounds, with a minor contribution of the C_{20}–C_{22} homologs. The chain length distribution is similar in most of the samples, though higher proportions of C_{27} compounds are observed in the samples from the Goguel Level at les Sauzeries and Glaise. Methylated triaromatic steroids are dominated by the C_{27}–C_{29} compounds, with a lesser proportion of C_{21} and C_{22} compounds. Compounds identification was made by comparison with previously published chro-

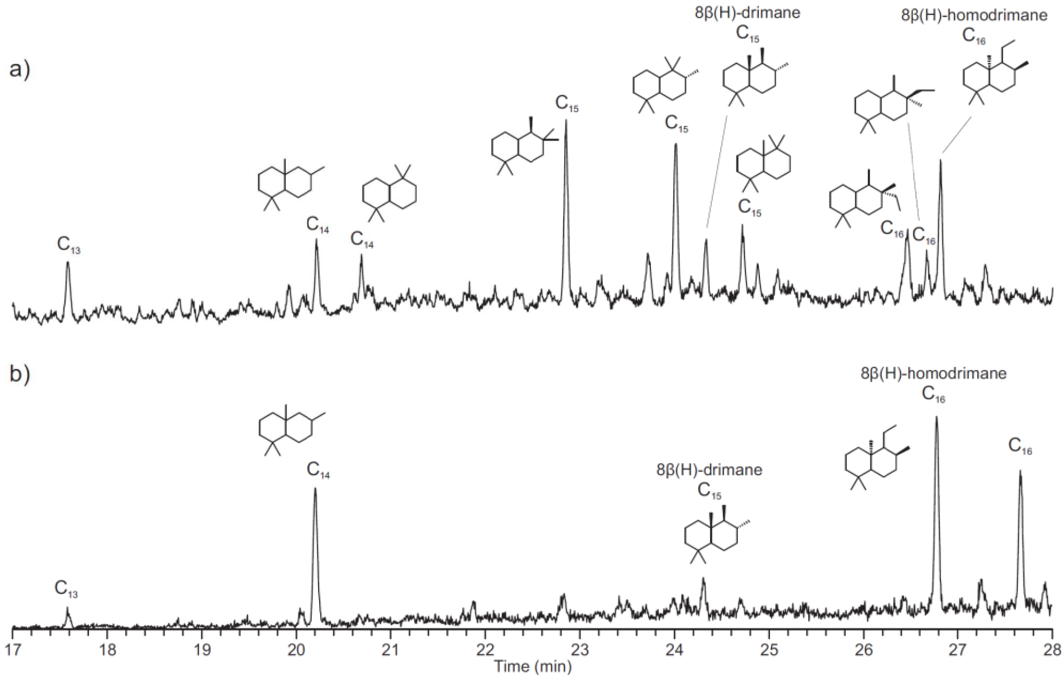

Supplementary Figure S8. Partial mass chromatogram m/z 123 + 165 + 179 + 193 + 207 showing typical distributions of bicyclic terpanes. (a) Sample SAUZOG006—Paquier Level; (b) sample SCOG012—Niveau Noir.

matograms [Ando et al., 2017]. The methylated triaromatic steroids correspond to 2-, 3- and 4-methyl isomers, as well as triaromatic dinosteroids. In most of the samples, the distribution is dominated by the 4-methyl isomers, with the C_{28} 4-methyl-20S-triaromatic steroid as the dominant compound (Supplementary Figure S10). Nevertheless, increased proportion of 2- and 3-methyl-isomers are observed in the samples from the Goguel Level at les Sauzeries and Glaise. The relative proportion of triaromatic dinosteroids is the highest in the samples from the Goguel Level at Notre-Dame and Saint Jaume. High proportions are also noted in the samples of the Paquier Level (Supplementary Table 1).

7. Other aromatic terpenoids

Mass chromatogram m/z 365 displays two series of compounds (Supplementary Figure S11). A first series is observed in most of the samples. Compounds present the same mass spectra as in Hussler et al. [1984] and corresponds to C_{29}–C_{31} aromatic 8,14-secohopanoids. The second series of compounds, eluting slightly after those of the first series, is observed in most of the samples except at Glaise and les Sauzeries sections (Supplementary Figure S11). Because of coelutions, the mass spectra of this second series of compounds are not clear. Nevertheless, it is surmised that they correspond to stereomers of the aromatic 8,14-secohopanoids previously described.

The aromatic terpenoids retene, cadalene, and 6-isopropyl-1-isohexyl-2-methylnaphthalene (ip-iHMN) are detected in most of the samples. By using the approach of van Aarssen et al. [2000], where the relative proportion of the three compounds is based on the mass chromatogram m/z 183+197+219, cadalene is dominant in all the samples. Its relative abundance is to 80% in most of the samples, except for the Goguel Level at les Sauzeries, where it is close to 50%. The relative abundance of these compounds is maximum in the marl samples from Pré-Guittard and minimum in the Goguel Level at Glaise and les Sauzeries (Supplementary Table 1). High relative abundances are also observed in the Paquier Level (Supplementary Table 1).

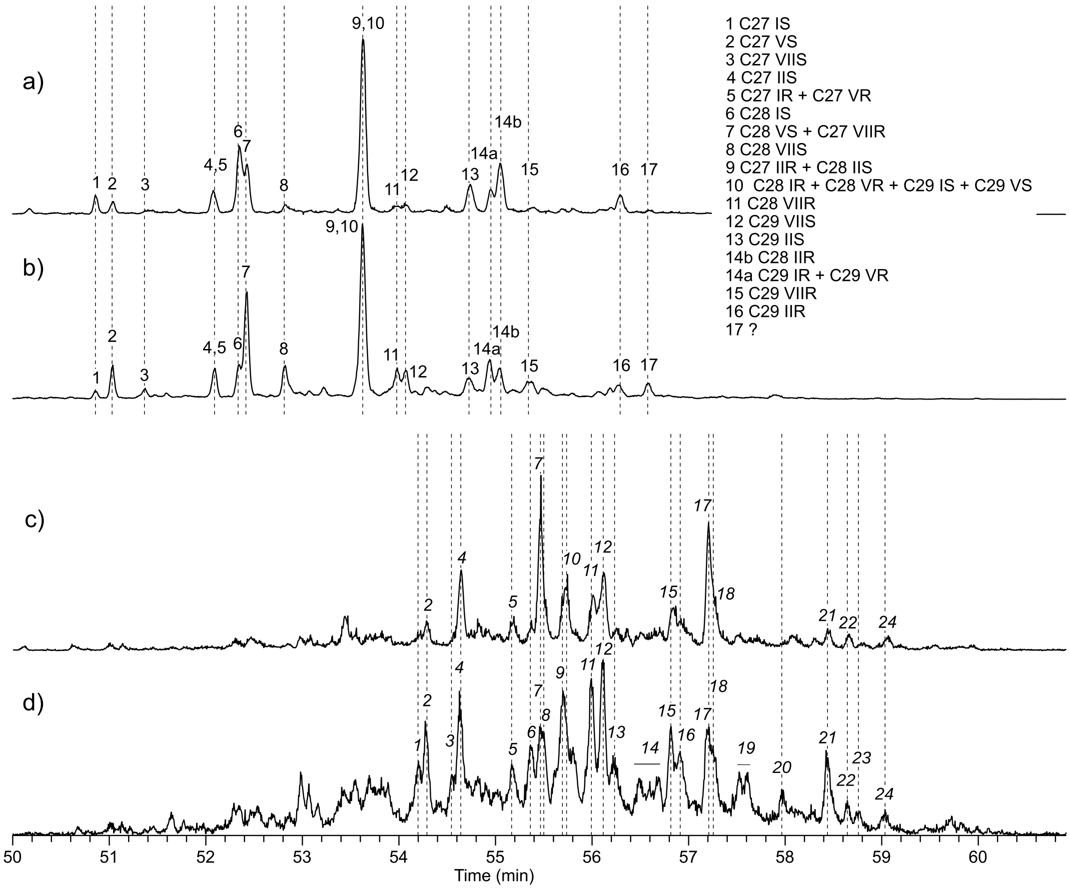

Supplementary Figure S9. Partial mass chromatograms showing the distribution of (a,b) ring-C monoaromatic steroids, m/z 253 and (c,d) ring-C monoaromatic methyl steroids, m/z 267, in the aromatic fraction of two selected samples. (a,c): ARBOG002A, Paquier Level; (b,d): TAFE2OG001, marls close to the Jacob Level. Compounds identification for (a) and (b) according to Riolo et al. [1986]. Compounds were not identified in (c) and (d).

Several aromatic terpenoids previously described [Hauke et al., 1993, 1992, Vliex et al., 1994] are observed in most of the samples: Des-E-D:C-friedo-25-norhopa-5,7,9-triene; D-methyl-des-E-D:C-friedo-25-norhopa-5,7,9-triene, 22,25,29,30-tetranor-18β-ferna-5,7,9-triene, 25-norarbora-5,7,9-triene (MAPH) and 5-methyl-10(4-methylpentyl)-des-A-25-norarbora(ferna)-5,7,9-triene (MATH). Their relative abundance is low and they are only detected through the selective detection of their characteristic ions.

Several benzohopanes are present in the aromatic fraction of most of the samples. These compounds mostly correspond to a series of C_{32}–C_{34} hopanes aromatised at C(20) detected using mass fragment m/z 191 (Hussler et al., 1984), as well as a C_{31} hopane aromatised at C(16) detected using mass fragment m/z 197 [Schaeffer et al., 1995]. In addition, a series of methylated benzohopanes, likely corresponding to 2 methyl-benzohopanes is detected in low proportion in several samples of the Goguel Level. The tetraaromatic hopane, 7-Methyl-3′-ethyl-1,2-cyclopentenochrysene [Wakeham et al., 1980] is also observed in most of the samples.

Series of methylated 2-methyl-(trimethyltridecyl)-chromans (MTTC) are observed in most of the samples, except samples from Pré-Guittard, les Sauzeries and Glaise sections. All four isomers generally

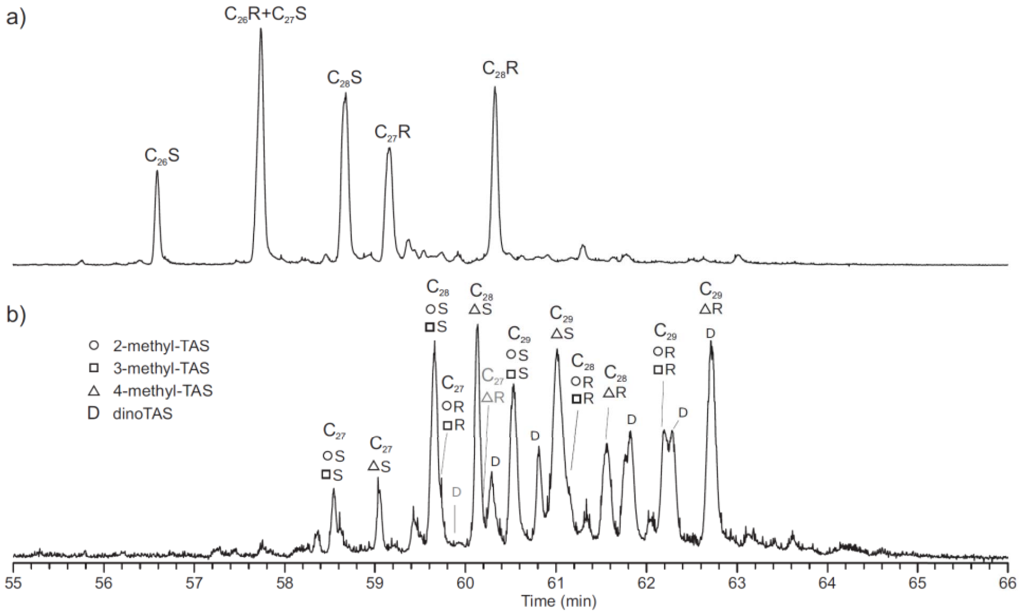

Supplementary Figure S10. Partial mass chromatograms showing the distribution of triaromatic steroids (TAS). (a) Non methylated TAS (m/z 231); (b) methylated-TAS (m/z 245). Sample GLEROG004 (Goguel Level, Glaise). Grey symbol indicates the compound is minor.

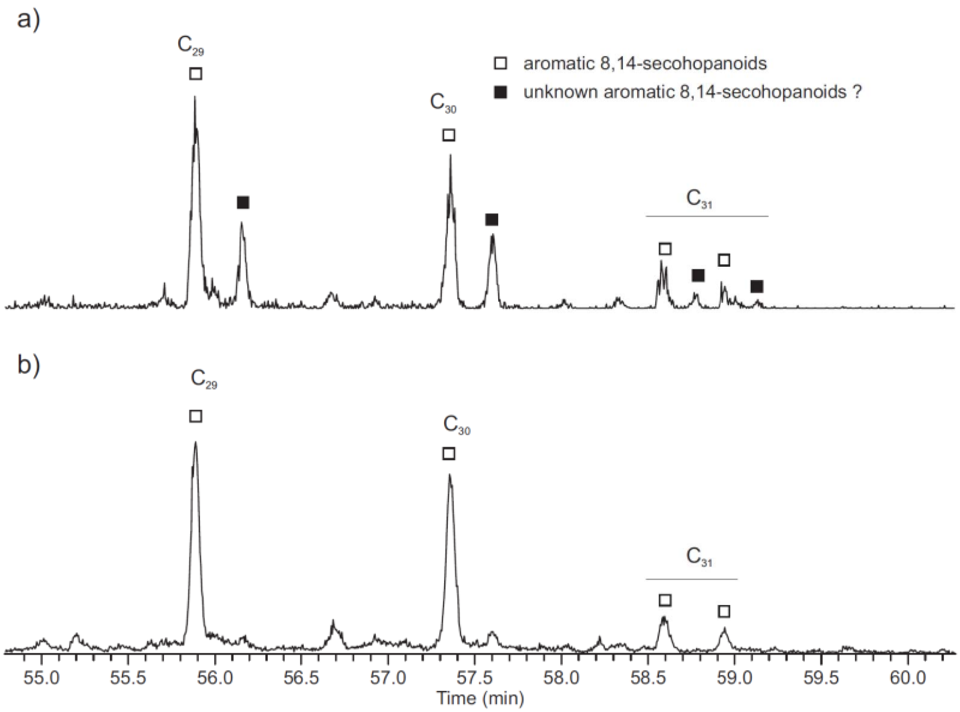

Supplementary Figure S11. Partial mass chromatogram m/z 365 showing the distribution of aromatic 8,14-secohopanoids in two selected samples. (a) Samples SJ2OG003, Goguel Level, Saint Jaume; (b) sample SAUZOG001, Goguel Level, les Sauzeries.

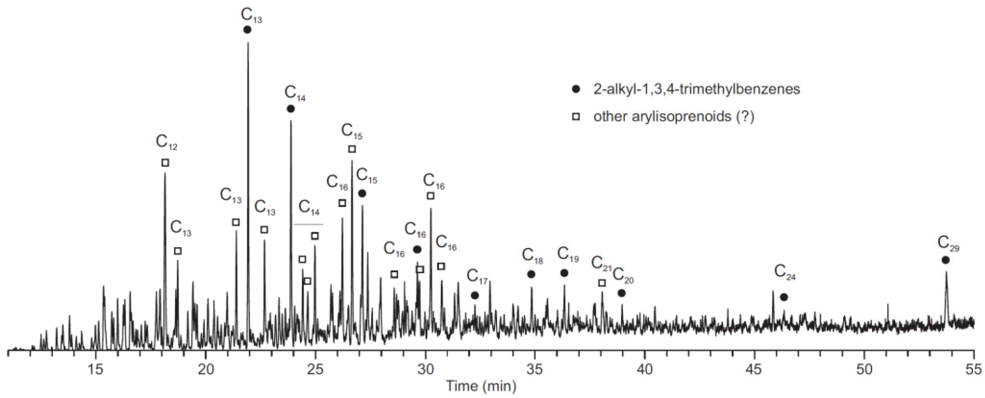

Supplementary Figure S12. Partial mass chromatogram m/z 133 + 134 showing a typical distribution of aryl isoprenoids. Sample SAUZOG001, Goguel Level, les Sauzeries.

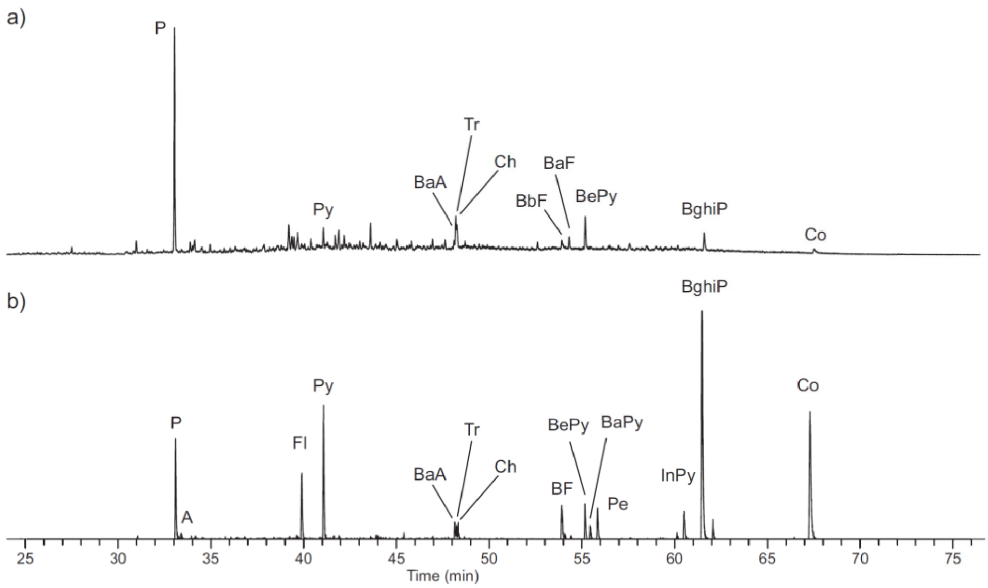

Supplementary Figure S13. Partial mass chromatogram m/z 178 + 202 + 228 + 252 + 276 + 300 showing typical distributions of PAHs. (a) Sample SAUZOG001-Goguel Level, les Sauzeries; (b) sample SCOG004, Fallot Interval. P: phenanthrene, A: anthracene, Fl: fluoranthene, Py: pyrene, BaA: benzo[*a*]anthracene, Tr: triphenylene, Ch: chrysene, BF: benzofluoranthenes, BaF: benzo[*a*]fluoranthene, BbF: benzo[*b*]fluoranthenes, BaPy: benzo[*a*]pyrene, BePy: benzo[*e*]pyrene, Pe: perylene, InPy: indeno[1,2,3-*cd*]pyrene, BghiP: benzo[*g*,*h*,*i*]perylene, Co: coronene.

described [Sinninghe Damsté et al., 1987] are present, nevertheless the 5,7,8-trimethyl-isomer is largely dominant, often representing more than 85%.

Aryl isoprenoids are detected in most of the organic levels, though generally in low abundance. This series ranges from C_{13} to C_{20}, with the C_{24} and C_{29} compounds also often present in low proportion (Supplementary Figure S12). Values of the aryl isoprenoid ratio [AIR; Schwark and Frimmel, 2004] are generally higher that 1, reflecting the dominance of short aryl isoprenoids (C_{13}–C_{15}); nevertheless, AIR values are lower than 1.0 in the Paquier Level. The highest proportions of aryl isoprenoids are observed in the Paquier Level, as well as the Goguel Level at Glaise and Notre-Dame (Supplementary Table 1). Several series of other substituted alkylben-

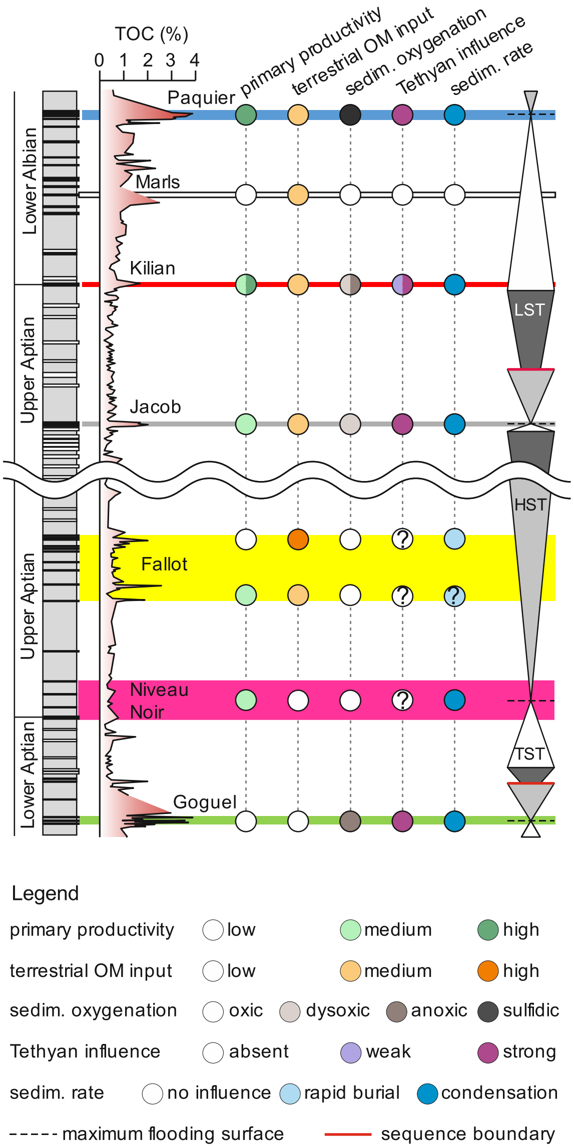

Supplementary Figure S14. Synthesis of factors and processes which controlled the OM sedimentation in the Blue Marls Formation based on biomarkers and previous analyses [Caillaud et al., 2022, 2020]. Lithostratigraphic column modified from Herrle et al. [2010]; synthetic TOC curve from Bréhéret [1995]; sequence stratigraphic framework derived from Rubino [1989; pers. comm., 2018] and Friès and Parize [2003]. TST: transgressive system tract, HST: highstand system tract; LST: lowstand system tract.

zenes ranging between C_{12} and C_{31} are also observed in most of the samples, but their substitution pattern could not be determined (Supplementary Figure S12). These compounds are particularly present in the Paquier Level.

8. Polycyclic aromatic hydrocarbons

Condensed polycyclic aromatic hydrocarbons (PAHs) were detected using mass fragments m/z 178 (phenanthrene and anthracene), 202 (fluoranthene and pyrene), 228 (naphthacene, benzo[*a*]anthracene chrysene, and triphenylene), 252 (benzofluoranthenes, benzopyrenes, and perylene), 276 (indeno[1,2,3-*c*,*d*]pyrene and benzo[*g*,*h*,*i*]perylene) and 300 (coronene). PAHs are present in most of the samples and show variable distributions. The highest relative abundances of PAHs are observed in the samples from Preguitard (marls), Tarandol (Kilian and Jacob levels), and Serre Chaitieu sections (Fallot Interval), where the dominant compounds are benzopyrene and coronene (Supplementary Figure S13). Low relative abundances are observed in the samples of the Goguel Level, Niveau Noir and Paquier Level, where the dominant compounds are phenanthrene and pyrene (Supplementary Figure S13).

Dibenzofuran is detected in most of the samples, except the marls from Pré-Guittard. Its highest abundance is observed in the Niveau Noir. Though this compound can have a pyrogenic origin similarly to the other PAHs, dibenzofuran and its alkylated counterparts have been related to lichens and can be used as tracers of terrigenous inputs [Radke et al., 2000]. Nevertheless, our data suggest that dibenzofuran here results from the degradation of an algal or microbial biomass (see main text).

9. Sulfur containing compounds

Organo-sulfur compounds (OSCs) are present in significant proportion in all the samples from the Paquier Level. They mostly correspond to a C_{20} isoprenoid thiophene (2,3-dimethyl-5-(2,6,10-trimethylundecyl)-thiophene) [Sinninghe Damsté et al., 1986] and several isomers of C_{20} isoprenoid benzothiophenes. The dominant compound is 2-(3,7-dimethyloctyl)-3,6-dimethylbenzo[*b*]thiophene [Sinninghe Damsté and de Leeuw, 1987]. OSCs are not observed in the other levels.

References

Ait-Itto, F.-Z., Martinez, M., Deconinck, J.-F., and Bodin, S. (2023). Astronomical calibration of the OAE1b from the Col de Pré-Guittard section (Aptian–Albian), Vocontian Basin, France. *Cret. Res.*, 150, article no. 105618.

Ando, T., Sawada, K., Okano, K., Takashima, R., and Nishi, H. (2017). Marine primary producer community during the mid-Cretaceous oceanic anoxic events (OAEs) 1a, 1b and 1d in the Vocontian Basin (SE France) evaluated from triaromatic steroids in sediments. *Org. Geochem.*, 106, 13–24.

Ando, T., Sawada, K., Okano, K., Takashima, R., and Nishi, H. (2022). Marine paleoecological variations during the mid-Cretaceous oceanic anoxic event 1a in the Vocontian Basin, southeastern France. *Palaeogeogr. Palaeoclimatol. Palaeoecol.*, 586, article no. 110779.

Benamara, A., Charbonnier, G., Adatte, T., Spangenberg, J. E., and Föllmi, K. B. (2020). Precession-driven monsoonal activity controlled the development of the early Albian Paquier oceanic anoxic event (OAE1b): evidence from the Vocontian Basin, SE France. *Palaeogeogr. Palaeoclimatol. Palaeoecol.*, 537, article no. 109406.

Bourbonniere, R. A. and Meyers, P. A. (1996). Sedimentary geolipid records of historical changes in the watersheds and productivities of Lakes Ontario and Erie. *Limnol. Oceanogr.*, 41, 352–359.

Bray, E. E. and Evans, E. D. (1961). Distribution of *n*-paraffins as a clue to recognition of source beds. *Geochim. Cosmochim. Acta*, 22, 2–15.

Bréhéret, J.-G. (1995). L'Aptien et l'Albien de la Fosse vocontienne (des bordures au bassin). Évolution de la sédimentation et enseignements sur les évenements anoxiques. Thèse de doctorat. Université François Rabelais—Tours.

Brocks, J. J., Buick, R., Logan, G. A., and Summons, R. E. (2003). Composition and syngeneity of molecular fossils from the 2.78 to 2.45 billion-year-old Mount Bruce Supergroup, Pilbara Craton, Western Australia. *Geochim. Cosmochim. Acta*, 67, 4289–4319.

Caillaud, A., Quijada, M., Hlohowskyj, S. R., Chappaz, A., Bout-Roumazeilles, V., Reynaud, J.-Y., Riboulleau, A., Baudin, F., Adatte, T., Ferry, J.-N., and Tribovillard, N. (2022). Assessing controls on organic matter enrichments in hemipelagic marls of the Aptian-Lower Albian Blue Marls of the Vocontian Basin (France): an unexpected variability observed from multiple "organic-rich" levels. *BSGF—Earth Sci. Bull.*, 193, article no. 2.

Caillaud, A., Quijada, M., Huet, B., Reynaud, J.-Y., Riboulleau, A., Bout-Roumazeilles, V., Baudin, F., Chappaz, A., Adatte, T., Ferry, J.-N., and Tribovillard, N. (2020). Turbidite-induced re-oxygenation episodes of the sediment-water interface in a diverticulum of the Tethys Ocean during the Oceanic Anoxic Event 1a: The French Vocontian Basin. *Depos. Rec.*, 6, 352–382.

Chen, J. and Summons, R. E. (2001). Complex patterns of steroidal biomarkers in Tertiary lacustrine sediments of the Biyang Basin, China. *Org. Geochem.*, 32, 115–126.

Friès, G. (1986). Dynamique du bassin subalpin à l'Apto-Cénomanien. These de doctorat, Paris 6 - Paris.

Friès, G. and Parize, O. (2003). Anatomy of ancient passive margin slope systems: Aptian gravity-driven deposition on the Vocontian palaeomargin, western Alps, south-east France. *Sedimentology*, 50, 1231–1270.

Hauke, V., Graff, R., Wehrung, P., Trendel, J. M., Albrecht, P., Riva, A., Hopfgartner, G., Gulacar, F. O., Buchs, A., and Eakin, P. A. (1992). Novel triterpene-derived hydrocarbons of the arborane/fernane series in sediments: Part II. *Geochim. Cosmochim. Acta*, 56, 3595–3602.

Hauke, V., Wehrung, P., Hussler, G., Trendel, J. M., Albrecht, P., Riva, A., and Connan, J. (1993). Rearranged des-E-hopanoid hydrocarbons in sediments and petroleum. *Org. Geochem.*, 20, 415–423.

Heimhofer, U., Hochuli, P. A., Herrle, J. O., and Weissert, H. (2006). Contrasting origins of Early Cretaceous black shales in the Vocontian basin: evidence from palynological and calcareous nannofossil records. *Palaeogeogr. Palaeoclimatol. Palaeoecol.*, 235, 93–109.

Herrle, J. O., Kössler, P., and Bollmann, J. (2010). Palaeoceanographic differences of early Late Aptian black shale events in the Vocontian Basin (SE France). *Palaeogeogr. Palaeoclimatol. Palaeoecol.*, 297, 367–376.

Hussler, G., Connan, J., and Albrecht, P. (1984). Novel families of tetra- and hexacyclic aromatic hopanoids predominant in carbonate rocks and crude oils. *Org. Geochem.*, 6, 39–49.

Kennedy, J., Gale, A., Huber, B., Petrizzo, M. R., Bown, P., and Jenkyns, H. (2017). The Global Boundary Stratotype Section and Point (GSSP) for the base of the Albian Stage, of the Cretaceous, the Col de Pré-Guittard section, Arnayon, Drôme, France. *Episodes*, 40, 177–188.

Meunier-Christmann, C., Albrecht, P., Brassell, S. C., Ten Haven, H. L., Van Der Linden, B., Rullkötter, J., and Trendel, J. M. (1991). Occurrence of dammar-13(17)-enes in sediments: indications for a yet unrecognized microbial constituent? *Geochim. Cosmochim. Acta*, 55, 3475–3483.

Moldowan, J. M., Seifert, W. K., and Gallegos, E. J. (1985). Relationship between petroleum composition and depositional environment of petroleum source rocks. *AAPG Bull.*, 69, 1255–1268.

Noble, R. A. (1986). *A Geochemical Study of Bicyclic Alkanes and Diterpenoid Hydrocarbons in Crude Oils, Sediments and Coals.* Curtin University of Technology, Perth, Western Australia.

Peters, K. E. and Moldowan, J. M. (1991). Effects of source, thermal maturity, and biodegradation on the distribution and isomerization of homohopanes in petroleum. *Org. Geochem.*, 17, 47–61.

Peters, K. E., Walters, C. W., and Moldowan, J. M. (2005). *The Biomarker Guide.* Cambridge University Press, Cambridge, 2nd edition.

Radke, M., Vriend, S. P., and Ramanampisoa, L. R. (2000). Alkyldibenzofurans in terrestrial rocks: influence of organic facies and maturation. *Geochim. Cosmochim. Acta*, 64, 275–286.

Radke, M., Welte, D. H., and Willsch, H. (1982a). Geochemical study on a well in the Western Canada Basin: relation of the aromatic distribution pattern to maturity of organic matter. *Geochim. Cosmochim. Acta*, 46, 1–10.

Radke, M., Willsch, H., Leythaeuser, D., and Teichmüller, M. (1982b). Aromatic components of coal: relation of distribution pattern to rank. *Geochim. Cosmochim. Acta*, 46, 1831–1848.

Reichelt, K. (2005). *Late Aptian-Albian of the Vocontian Basin (SE-France) and Albian of NE-Texas: Biostratigraphic and paleoceanographic implications by planktic foraminifera faunas.* PhD thesis, Eberhard-Karls-Universität, Tübingen.

Riolo, J., Hussler, G., Albrecht, P., and Connan, J. (1986). Distribution of aromatic steroids in geological samples: their evaluation as geochemical parameters. *Org. Geochem.*, 10, 981–990.

Rubino, J. L. (1989). Introductory remarks on Upper Aptian to Albian siliciclastic/carbonate depositional sequences. In Ferry, S. and Rubino, J. L., editors, *Mesozoic Eustacy on Western Tethyan Margins. Post-Meeting Field Trip in the "Vocontian Trough"*, pages 28–45. ASF Publications Spéciales, Paris.

Scalan, E. S. and Smith, J. E. (1970). An improved measure of the odd-even predominance in the normal alkanes of sediment extracts and petroleum. *Geochim. Cosmochim. Acta*, 34, 611–620.

Schaeffer, P., Adam, P., Trendel, J.-M., Albrecht, P., and Connan, J. (1995). A novel series of benzohopanes widespread in sediments. *Org. Geochem.*, 23, 87–89.

Schwark, L. and Frimmel, A. (2004). Chemostratigraphy of the Posidonia Black Shale, SW-Germany: II. Assessment of extent and persistence of photic-zone anoxia using aryl isoprenoid distributions. *Chem. Geol.*, 206, 231–248.

Sinninghe Damsté, J. S. and de Leeuw, J. W. (1987). The origin and fate of isoprenoid C_{20} and C_{15} sulphur compounds in sediments and oils. *Int. J. Environ. An. Chem.*, 28, 1–19.

Sinninghe Damsté, J. S., Kock-van Dalen, A. C., de Leeuw, J. W., Schenck, P. A., Guoying, S., and Brassel, S. C. (1987). The identification of mono-, di- and trimethyl 2-methyl-(4,8,12)-trimethyldecyl)chromans and their occurrence in the geosphere. *Geochim. Cosmochim. Acta*, 51, 2393–2400.

Sinninghe Damsté, J. S., ten Haven, H. L., de Leeuw, J. W., and Schenck, P. A. (1986). Organic geochemical studies of a Messinian evaporitic basin, northern Apennines (Italy). II. Isoprenoid and *n*-alkyl thiophenes and thiolanes. *Org. Geochem.*, 10, 791–805.

Summons, R. E. and Jahnke, L. L. (1990). Identification of the methylhopanes in sediments and petroleum. *Geochim. Cosmochim. Acta*, 54, 247–251.

Tribovillard, N.-P. and Gorin, G. E. (1991). Organic facies of the Early Albian Niveau Paquier, a key black shales horizon of the Marnes Bleues formation in the Vocontian trough (Subalpine Ranges, SE France). *Palaeogeogr. Palaeoclimatol. Palaeoecol.*, 85, 227–237.

van Aarssen, B. G. K., Alexander, R., and Kagi, R. I. (2000). Higher plant biomarkers reflect palaeovegetation changes during Jurassic times. *Org. Geochem.*, 64, 1417–1424.

Vink, A., Schouten, S., Sephton, S., and Sinninghe Damsté, J. S. (1998). A newly discovered norisoprenoid, 2,6,15,19-tetramethylicosane, in Cretaceous black shales. *Geochim. Cosmochim. Acta*, 62, 965–970.

Vliex, M., Hagemann, H. W., and Püttmann, W. (1994). Aromatized arborane/fernane hydrocarbons as molecular indicators of floral changes in Upper Carboniferous/Lower Permian strata of the Saar-Nahe Basin, southwestern Germany. *Geochim. Cosmochim. Acta*, 58, 4689–4702.

Wakeham, S. G., Schaffner, C., and Giger, W. (1980). Polycyclic aromatic hydrocarbons in Recent lake sediments—I. Compounds having anthropogenic origins. *Geochim. Cosmochim. Acta*, 44, 403–413.

Wang, T. G., Simoneit, B. R. T., Philp, R. P., and Yu, C. P. (1990). Extended 8β(H)-drimane and 8,14-secohopane series in a Chinese boghead coal. *Energy Fuels*, 4, 177–183.